Short communication

An articular cartilage contact model based on real surface geometry

Sang-Kuy Han[a], Salvatore Federico[b], Marcelo Epstein[a], Walter Herzog[c],*

[a] *Department of Mechanical and Manufacturing Engineering, The University of Calgary, 2500 University Drive NW, Calgary, Alberta T2N 1N4, Canada*
[b] *Department of Industrial and Mechanical Engineering, University of Catania, Viale Andrea Doria 6, Catania 95125, Italy*
[c] *Human Performance Laboratory, Faculty of Kinesiology, The University of Calgary, 2500 University Drive NW, Calgary, Alberta T2N 1N4, Canada*

Abstract

Abnormal, excessive stresses acting on articular joint surfaces are speculated to be one of the causes for joint degeneration. However, articular surface stresses have not been studied systematically, since it is technically difficult to measure in vivo contact areas and pressures in dynamic situations. Therefore, we implemented a numerical model of articular surface contact using accurate surface geometries. The model was developed for the cat patellofemoral joint. We demonstrated that small misalignments of the patella relative to the femur change the joint contact mechanics substantially for a given external load. These results suggest that misalignment might be studied as one of the factors causing articular cartilage disorder and joint degeneration.
© 2004 Elsevier Ltd. All rights reserved.

1. Introduction

Articular cartilage is subjected to a wide range of mechanical stresses associated with normal, everyday joint loading in vivo, and it is known to become injured or diseased frequently in the human knee, particularly in athletes and the elderly (Baker et al., 1985; Smillie, 1970; Lawrence et al., 1989).

Abnormal or excessive stresses acting on, or within, a joint are speculated to be one of the causes for patellofemoral joint degeneration (Radin et al., 1978; Moskowitz, 1992). Support for this idea comes from experiments in which cartilage degeneration has been initiated in animals by excessive loading (Dekel and Weissman, 1978; Moskowitz, 1992).

At present, the in vivo joint contact mechanics cannot be measured in diarthrodial joints during voluntary movements, although dynamic contact pressure measurements in artificial joints (e.g., Bergmann et al., 1993), and static conditions in intact diarthrodial joints have been made (e.g., Ronsky et al., 1995). Further-

more, studies performed on cartilage explants cannot explain the stress–strain states of articular cartilage subjected to loads in the intact joint, because of the artificial boundary conditions required for in vitro testing (e.g., no interaction with the subchondral bone, and either completely open or completely sealed lateral constraints). Also, the biological response of articular cartilage to loading performed in isolated explants in vitro, or in the intact joint, can be very different for apparently similar loading conditions (Craig, 2003; Clark et al., 2004). Therefore, theoretical approaches of accurate joint contact mechanics are urgently needed. However, exact analytical solutions can only be obtained for small displacements and two-dimensional (2-D), or axisymmetric and simple geometries (Athesian et al., 1994; Wu et al., 1997). When studying real joint geometries, a numerical analysis, such as the finite element (FE) method, is necessary. The purpose of this study was to combine an accurate geometrical representation of a real joint with a numerical approach of the associated contact mechanics. In order to do this, we used the cat patellofemoral joint for which in situ contact pressure measurements had been made in the past (Clark et al., 2002). We then simulated lateral patellar shifts of 0.5 and 1.0 mm from the actual in situ

---

*Corresponding author. Tel.: +1-403-220-8525; fax: +1-403-284-3553.

E-mail address: walter@kin.ucalgary.ca (W. Herzog).

alignment. We hypothesized that these misalignments were associated with increased peak pressure, decreased contact area, higher tensile stresses at the articular surface, and higher shear stresses at the bone–cartilage interface, for a given contact force. Such observations would be consistent with anecdotal and clinical findings of increased patellofemoral degeneration with inaccurate patellar tracking.

2. Methods

Accurate ($<20 \mu m$) retropatellar and femoral groove surface geometries were obtained using laser scanning (MicroScan Laser Profilometer, LMI Technologies, Southfield, MI, USA) (Haut et al., 1998; Couillard, 2002). The 3-D FE mesh model was created using the commercial mesh generation software, TrueGRID (Fig. 1a and b). A large displacement contact analysis was used with ABAQUS 6.3. Articular cartilage was assumed to be biphasic: the solid phase was assumed linearly elastic and incompressible, and the fluid phase was taken as incompressible, non-viscous, and with a deformation-dependent permeability (Holmes and Mow, 1990). The deformation dependent permeability was described by Wu and Herzog (2000) as a function of the void ratio e (ratio of the fluid over the solid fraction):

$$k = \left(\frac{e}{e_0}\right)^{\kappa} \exp\left(\frac{M}{2}\left[\left(\frac{1+e}{1+e_0}\right)^2 - 1\right]\right). \qquad (1)$$

The elastic constants and the material parameters featuring in the expression of permeability (Eq. (1)) were taken from the literature (Wu et al., 1999; Wu and Herzog, 2000), and are shown in Table 1.

The articular cartilage surface was assumed perfectly permeable, and cartilage thickness on the femoral groove and retropatellar surface was approximated as 0.3 and 0.5 mm, respectively (Herzog et al., 1998). The articular cartilage was modeled as being attached to a cortical bone of 2.5 mm thickness. In order to evaluate
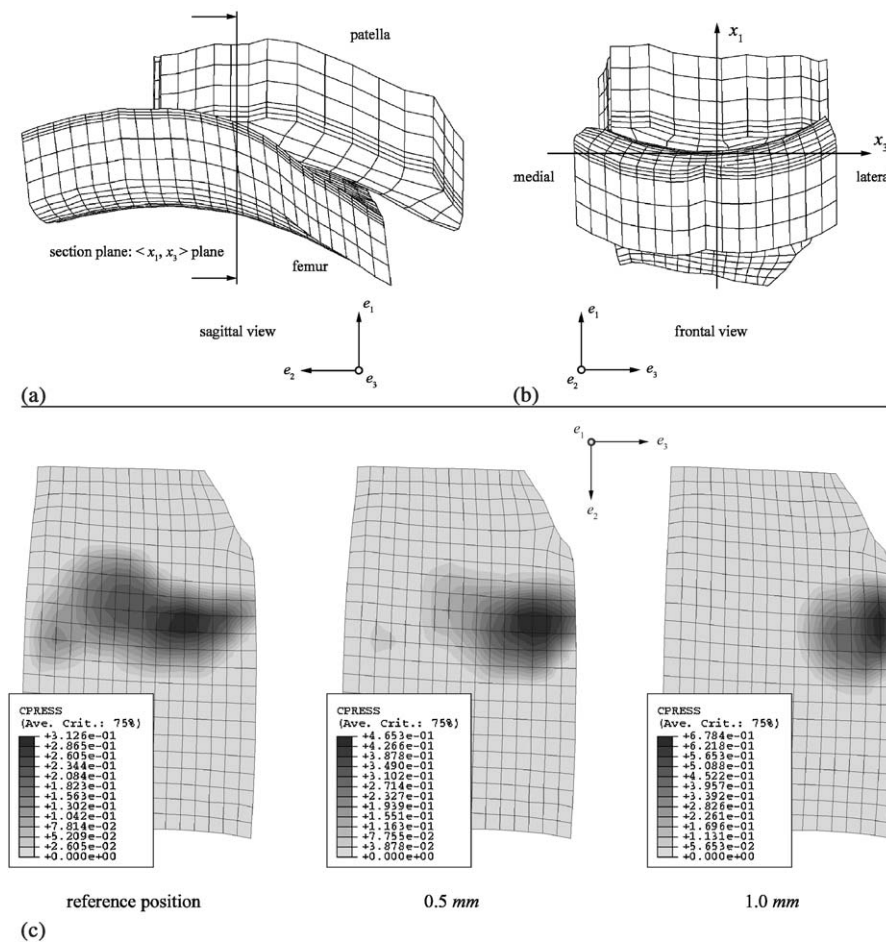
Fig. 1. Patellofemoral joint contact mesh model: (a) sagittal view, with the section plane on which the local contact pressure was evaluated; (b) frontal view, with the reference frame; and (c) contact pressure distribution for a 3 N applied load with the patella in the normal reference position, and displaced laterally by 0.5 and 1.0 mm.

Table 1
Material properties used in the simulations

Material properties		Values
Cartilage layer		
Young's modulus	E	0.450 MPa
Poisson's ratio	v	0.106
Initial permeability	K_0	$1.16 \times 10^{-3}\,\mathrm{mm^4\,N^{-1}\,s^{-1}}$
Initial void ratio	e_0	4.2
Material parameters for the $k-e$ relationship	M	4.638
	κ	0.0848
Bone layer		
Young's modulus	E	$2 \times 10^3\,\mathrm{MPa}$
Poisson's ratio	v	0.20

the effects of alignment of the patella relative to the femur, the patella was shifted laterally by 0.5 and 1.0 mm from its reference configuration. Ramp loads from 0 to 3, 100, 150, and 500 N were applied over a 2 s period to the patella placed on the femoral groove.

Analysis: Patellofemoral contact areas, peak pressures, and local pressures were calculated and compared for the four loading conditions (ramp to 3, 100, 150, and 500 N), and the three positions of the patella relative to the femur (normal reference position, 0.5 and 1.0 mm lateral displacement of the patella relative to the femur). Contact area was defined as the area spanned by the nodes of the FE model in which contact pressure was non-zero. Peak pressure was defined as the peak pressure observed at the end of the loading ramp. Local pressures were analyzed along three parallel lines running from medial to lateral through the peak pressure point, and ± 0.25 mm distal and proximal to the peak pressure point, respectively. The maximum tensile stress was calculated as the maximum value of the principal stresses (i.e., the three eigenvalues of the stress tensor). The maximum shear stress was calculated as half of the maximum Tresca equivalent stress:

$$\tau_{\max} = \tfrac{1}{2}(\sigma_{\mathrm{eq}}^{\mathrm{Tresca}})_{\max}$$
$$= \tfrac{1}{2}[\max\{|\sigma_1 - \sigma_2|, |\sigma_1 - \sigma_3|, |\sigma_2 - \sigma_3|\}]_{\max}, \quad (2)$$

where σ_1, σ_2, σ_3 are the principal stresses.

3. Results

In the normal reference position, the patellofemoral contact area extended from the medial to the lateral side of the femoral groove, as observed experimentally (Clark et al., 2002). For a 0.5 and 1.0 mm lateral shift of the patella from its reference position, the contact areas and peak pressures were shifted laterally (Fig. 1c). Also, contact area decreased and peak contact pressure

increased with a lateral shift of the patella for all loading conditions (Fig. 2). We also calculated the contact pressures on the femur at the points lying on the intersection of the surface with the section plane shown in Fig. 1a, and plotted the results with respect to the local x_3 coordinate of the contact points (Fig. 1b). Compared to the normal reference position, local loading of the laterally displaced patellar positions caused unloading medially and overloading laterally (Fig. 3).

Theoretically predicted peak contact pressures were within the range of those observed experimentally (Fig. 4a), while contact areas were vastly overestimated by the numerical contact model (Fig. 4b).

Maximal tensile stresses always occur at the articular cartilage surface, and they remain fairly constant across different alignments of patella relative to femur. In
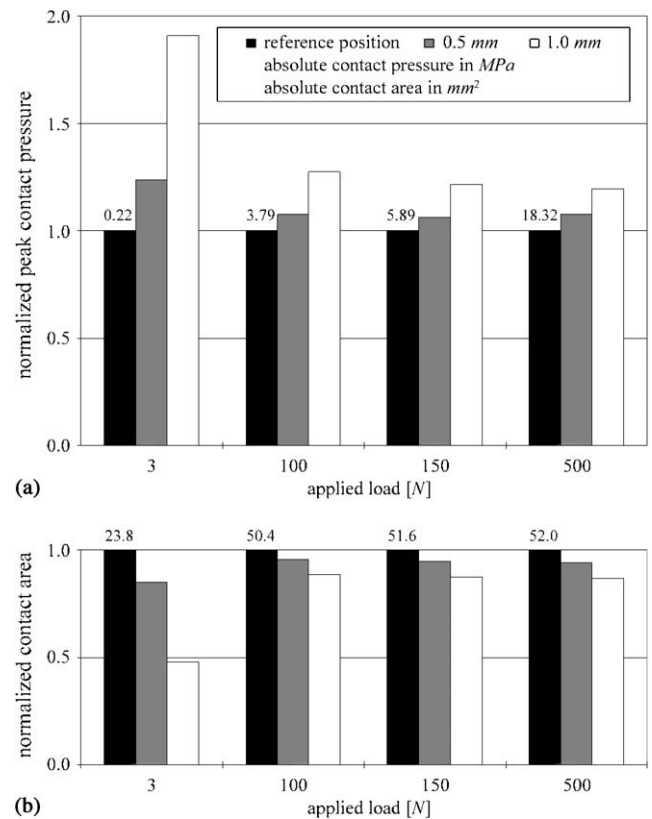
Fig. 2. (a) Normalized peak patellofemoral contact pressure for the four loading conditions (3, 100, 150, and 500 N) and the three positions of the patella relative to the femur (normal, 0.5 and 1.0 mm lateral displacement). Normalized peak pressures increase with increasing displacement of the patella from its reference position. (b) Normalized patellofemoral contact area for the four loading conditions (3, 100, 150, and 500 N) and the three positions of the patella relative to the femur (normal, 0.5 and 1.0 mm lateral displacement). Contact area increased dramatically from the 3 to 100 N loading conditions, but remained virtually constant for further increases in load magnitude. Contact area decreased with increasing patellar displacement from the reference position. The absolute values of contact pressure (in MPa) and contact area (in mm²) are reported for the reference configuration.
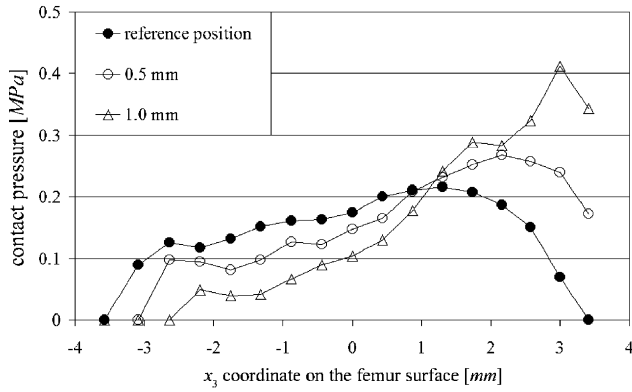
Fig. 3. Local contact pressures along a medial–lateral line for the three positions of the patella relative to the femur for the 3 N loading condition. Note, the lateral shift and increase in peak pressure with increasing lateral shifting of the patella. In this case, peak pressure from the normal reference to the 1.0 mm displaced position increased by a factor of 2.
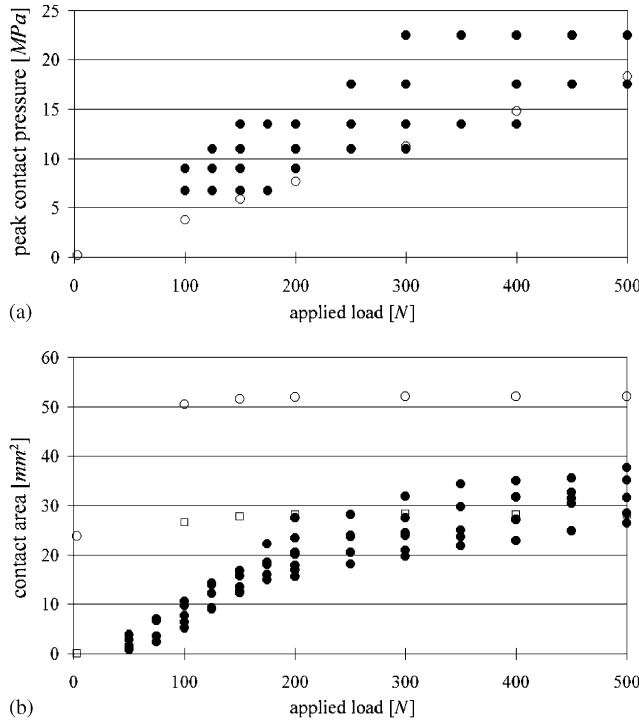
Fig. 4. (a) Comparison of peak contact pressure as a function of patellofemoral contact force (applied load) calculated theoretically ($\bigcirc$), and obtained experimentally ($\bullet$) from cat patellofemoral joints. (b) Comparison of patellofemoral contact area as a function of patellofemoral contact force (applied load) calculated theoretically ($\bigcirc$), and obtained experimentally ($\bullet$) from five cat patellofemoral joints. Theoretical contact areas were calculated for the whole contact area ($\bigcirc$), and for the whole contact minus 23.8 mm^2 ($\square$).

contrast, maximal shear stresses occur near the bone–cartilage interface, and they increase substantially with increasing misalignment of patella relative to femur (Fig. 5).
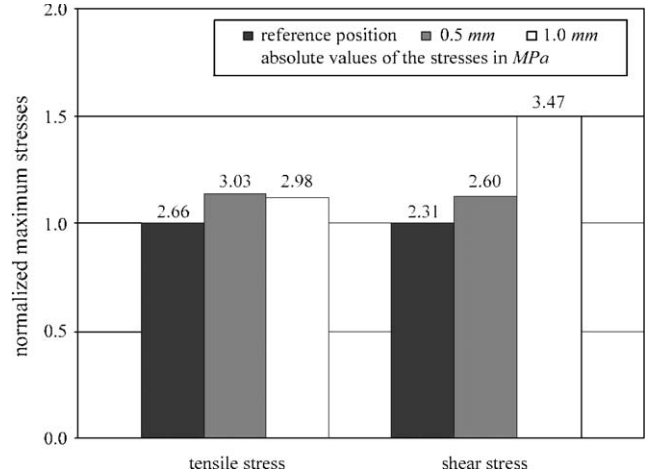
Fig. 5. Maximum tensile and shear stresses for the three alignment conditions of the patella relative to the femur (normal, 0.5 and 1.0 mm lateral displacement). The maximum tensile stress occurred at the articular surface and was not greatly affected by misalignment. The maximum shear stress occurred at the bone–cartilage interface and was significantly affected by misalignment.

4. Discussion

At present, it is impossible to determine experimentally the instantaneous, in vivo stress–strain state of articular cartilage during movement. However, there is increasing evidence that cartilage adaptation and degeneration are strongly linked to mechanical signals in the vicinity of the chondrocytes (Guilak et al., 1997). Therefore, we combined an accurate diarthrodial joint geometry (obtained through laser digitization) with a realistic (biphasic, strain-dependent permeability) contact model of articulating joint surfaces, implemented on a commercial FE platform. We applied physiologically occurring patellofemoral contact forces (Hasler and Herzog, 1998) to the model to obtain the corresponding contact area and contact pressure distributions. Of course, the complete stress–strain states of the articular cartilage in the current model, or a model containing structural elements, such as chondrocytes (Wu et al., 1999; Wu and Herzog, 2000) and/or collagen fibrils, (Li et al., 1999) could have been determined as well.

Comparison of the peak contact pressure data with experimental data was good, although the theoretically predicted pressures were at the lower limits of those obtained experimentally (Fig. 4a). However, this result could be caused by the difference in knee angles. The theoretically simulated knee angle was 70°, whereas the experimentally obtained results corresponded to a knee angle of 100°. Furthermore, peak pressure measurements using Fuji pressure sensitive film are not trivial and may contain errors of up to 30% associated with the

change in contact mechanics because of insertion of the Fuji film (Wu et al., 1998), possible crinkle artifacts (Liggins, 1997), and inaccuracies with Fuji film calibration (Liggins et al., 1995).

However, comparison of the contact areas obtained theoretically and experimentally might be of greater concern (Fig. 4b). The theoretically predicted contact areas were always substantially greater than the experimentally measured values. However, the experimental data were obtained with Fuji pressure sensitive film. This film has a threshold for pressure detection, in the case at hand, of about 2.0 MPa. At 3 N of applied load, the predicted peak contact pressure was 0.3 MPa, and the predicted contact area was 23.8 mm^2. Since the peak pressure in this case was below the Fuji film threshold, an experiment would have given a contact area of 0 mm^2 for the 3 N load application. This result indicates that the experimentally measured contact areas are likely underestimated compared to the actual contact areas. For example, if we subtract the known error at the 3 N load (i.e., 23.8 mm^2) from all contact areas shown in Fig. 4, the corrected values show good agreement with the experimental values, except for the 100 and 150 N load, for which the predicted values would still be too high (Fig. 4b), although we suspect, this result is caused by our assumption of a constant contact area measurement error of 23.8 mm^2.

Summarizing, we demonstrated that small changes in patellar displacement caused changes in contact area, peak pressure, and maximum shear stress near the bone–cartilage interface. However, these changes were not so dramatic that we might expect them to affect joint degeneration. Patellar misalignment also caused loaded of articular regions that were not part of the contact region in normal patellofemoral alignment (Fig. 3). We speculate that sudden loading of these normally unloaded regions might cause the problems associated with mal-tracking of the patella. This might explain the clinical observation that abnormal patellar tracking is associated with knee pain, and possibly, degenerative processes of the knee (Fulkerson and Shea, 1990). Finally, we note that, at least for the misalignments that were studied here (lateral shift of the patella), the maximum tensile stress at the contact surface was not significantly affected in intensity or direction.

References

Athesian, G.A., Lai, W.M., Zhu, W.B., Mow, V.C., 1994. An asymptotic solution for the contact of two biphasic cartilage layers. Journal of Biomechanics 27, 1347–1360.

Baker, B.E., Peckhan, A.C., Puppard, F., Sanborn, J.C., 1985. Review of meniscal injury and associated sports. The American Journal of Sports Medicine 13, 1–4.

Bergmann, G., Graichen, F., Rohlmann, A., 1993. Hip joint loading during walking and running, measured in two patients. Journal of Biomechanics 26, 969–990.

Clark, A.L., Herzog, W., Leonard, T.R., 2002. Contact area and pressure distribution in the feline patellofemoral joint under physiologically meaningful loading conditions. Journal of Biomechanics 35 (1), 53–60.

Clark, A.L., Mills, L., Hart, D.A., Herzog, W., 2004. Muscle-induced Joint Loading Rapidly Affects Cartilage mRNA Levels in a Site-specific Manner. Journal of Musculoskeletal Research 8 (1), 1–12.

Couillard, S., 2002. Cartilage deformation from laser scanning. M.Sc. Thesis, University of Calgary.

Craig, S., 2003. Effects of in-vivo joint loading on articular cartilage chondrocyte viability. M.Sc. Thesis, University of Calgary.

Dekel, S., Weissman, S.L., 1978. Joint changes after overuse and peak overloading of rabbit knees in vivo. Acta Orthopaedica Scandinavica 49 (6), 519–528.

Fulkerson, J.P., Shea, K.P., 1990. Mechanical basis for patellofemoral pain and cartilage breakdown. In: Ewing, J.W. (Ed.), In Articular Cartilage and Knee Joint Function: Basic Science and Arthroscopy. Raven Press, New York, pp. 93–101.

Guilak, F., Spilker, R.L., Setton, L.A., 1997. Physical regulation of cartilage metabolism. In: Mow, V.C., Hayes, W.C. (Eds.), Basic Orthopaedic Biomechanics. Lippincott-Raven, Philadelphia, pp. 179–207.

Hasler, E.M., Herzog, W., 1998. Quantification of in vivo patellofemoral contact forces before and after ACL transection. Journal of Biomechanics 31 (1), 37–44.

Haut, T.L., Hull, M.L., Howell, S.M., 1998. A high-accuracy three-dimensional coordinate digitizing system for reconstructing the geometry of diarthrodial joints. Journal of Biomechanics 31 (6), 571–577.

Herzog, W., Diet, S., Suter, E., Mayzus, P., Leonard, T.R., Müller, C., Wu, J.Z., Epstein, M., 1998. Material and functional properties of articular cartilage and patellofemoral contact mechanics in an experimental model of osteoarthritis. Journal of Biomechanics 31, 1137–1145.

Holmes, M.H., Mow, V.C., 1990. The non-linear characteristics of soft gels and hydrated connective tissues in ultrafiltration. Journal of Biomechanics 23, 1145–1156.

Lawrence, R.C., Hochberg, M.C., Kelsey, J.L., McDuffie, F.C., Medsger Jr., T.A., Felts, W.R., Shulman, L.E., 1989. Estimates of the prevalence of selected arthritic and musculoskeletal diseases in the United States. Journal of Rheumatology 16 (4), 427–441.

Li, L.P., Soulhat, J., Buschmann, M.D., Shirazi-Adl, A., 1999. Nonlinear analysis of cartilage in unconfined ramp compression using a fibril reinforced poroelastic model. Clinical Biomechanics 14, 673–682.

Liggins, A.B., 1997. The practical application of Fuji prescale pressure-sensitive film. In: Orr, J.F., Shelton, J.C. (Eds.), Optical Measurement Methods in Biomechanics. Chapman & Hall, London, pp. 173–189.

Liggins, A.B., Hardie, W.R., Finlay, J.B., 1995. The spatial and pressure resolution of Fuji pressure-sensitive film. Experimental Mechanics 35, 166–173.

Moskowitz, R.W., 1992. Experimental models of osteoarthrits. In: Moskowitz, R.W., Howell, D.S., Goldberg, V.M., Mankin, H.J.

(Eds.), Osteoarthritis: Diagnosis and Medical/Surgical Management, 2nd Edition. W.B. Saunders, Philadelphia, pp. 233–262.

Radin, E.L., Ehrlich, M.G., Chernack, R., 1978. Effect of repetitive impulsive loading on the knee joints of rabbits. Clinical Orthopaedics 131, 288–293.

Ronsky, J.L., Herzog, W., Brown, T.D., Pedersen, D.R., Grood, E.S., Butler, D.L., 1995. In-vivo quantification of the cat patellofemoral joint contact stresses and areas. Journal of Biomechanics 28, 977–983.

Smillie, I.S., 1970. Injuries of the Knee Joint 5th Edition. Williams &Wilkins, Baltimore.

Wu, J.Z., Herzog, W., 2000. Finite element simulation of location- and time-dependent mechanical behavior of chondrocytes in uncon-

fined compression tests. Annals of Biomedical Engineering 28, 318–330.

Wu, J.Z., Herzog, W., Epstein, M., 1997. An improved solution for the contact of two biphasic cartilage layers. Journal of Biomechanics 30, 371–375.

Wu, J.Z., Herzog, W., Epstein, M., 1998. Effects of inserting a pressensor film into articular joints on the actual contact mechanics. Journal of Biomechanical Engineering 120, 655–659.

Wu, J.Z., Herzog, W., Epstein, M., 1999. Modeling of location- and time-dependent deformation of chondrocytes during cartilage loading. Journal of Biomechanics 32, 563–572.